

Proceedings of the tenth international conference on liquid and amorphous metals, Dortmund, 1998, J. Non-Crystal. Solids, in press.

## X-RAY ABSORPTION FINE STRUCTURE STUDIES ON EXPANDED FLUID SE: FROM LIQUID TO DENSE VAPOR

M. Inui<sup>a</sup>, K. Tamura<sup>a</sup>, J. L. Hazemann<sup>b</sup>, D. Raoux<sup>b</sup>, Y. Soldo<sup>b</sup>, R. Argoud<sup>b</sup> and J. F. Jal<sup>c</sup>

<sup>a</sup> *Faculty of Integrated Arts and Sciences, Hiroshima University, Higashi-Hiroshima 739-8521, Japan*

<sup>b</sup> *Laboratory of Crystallography-CNRS, BP 166, 38042 Grenoble Cedex 09, France*

<sup>c</sup> *Department of Material Physics, Claude-Bernard University Lyon I, France*

### Abstract

X-ray absorption fine structure (XAFS) measurements for expanded fluid Se at high temperatures and pressures up to 1650 °C and 600bar have been carried out to investigate the change of local structure with volume expansion. The electronic property of fluid Se changes from a semiconducting one to metallic with increasing temperature and pressure. When the volume is further expanded, the fluid becomes non-metallic vapor. XAFS spectra of the non-metallic vapor shows that the vapor rarer than the critical density consists mainly of Se dimers. When the volume contracts exceeding the critical density, the first peak in the radial distribution function is shifted towards larger distance and is increasingly asymmetrical.

## 1 Introduction

Fluid (f-) Se undergoes a semiconductor-metal (SC-M) transition at high temperature and high pressure [1]. Many experimental and theoretical investigations have been made so far to understand the SC-M transition [2]–[13]. Recent experimental studies have suggested that the transition occurs around the contour of 30  $\Omega^{-1}\text{cm}^{-1}$ [8].

As is well known, liquid Se has two-fold coordinated chain structure and more

than  $10^4$  atoms are covalently bonded near the melting temperature. The result of nuclear magnetic resonance measurements [2] suggest that the average chain length becomes short with increasing temperature and pressure. Structural studies show that the two-fold coordinated structure is largely preserved in the metallic f-Se at high temperature and pressure [7, 9]. These data mean that the SC-M transition is connected to the stability of the chain structure. To observe the change of covalent bonds in the chain, x-ray absorption fine structure (XAFS) spectroscopy is a useful probe. It prompts us to carry out the XAFS measurements despite difficulties in experimental technique such as high pressure and high temperature. We have measured XAFS spectra of f-Se up to the metallic region and already reported structural change at the SC-M transition [10].

When the metallic fluid is further expanded, the conductivity decreases and the fluid finally becomes an insulating vapor consisting of Se dimers, which indicates that metal-non-metal (M-NM) transition occurs in the volume expansion process around the critical point (the critical constants;  $T_c=1615^\circ\text{C}$ ,  $p_c=385\text{bar}$  and  $\rho_c=1.85\text{g/cm}^3$  [12]). It is interesting to study how Se dimers condense to a metallic fluid consisting of chain molecules. Two of the authors carried out XAFS measurements for dense Se vapor to 150 bar at the Photon Factory [14] and studied the temperature and pressure variation of the covalent bond in a Se dimer. In this paper, results of XAFS measurements for pressure variation at  $1650^\circ\text{C}$  in addition to temperature variation at 600 bar are presented.

## 2 Experimental

XAFS measurements were carried out in transmission mode using the spectrometer installed by the French Collaborative Research Group on BM32 beamline at the ESRF. The details of the optics are described in a previous paper [10]. The experimental condition of high temperature and high pressure were achieved using an internally heated high-pressure vessel made of super- high-tension steel, similar to the previous one [14]. The incident and transmitted x-ray beams passed through Be windows. The vessel was pressurized by He gas (99.9999%). The Se sample (99.999

%) was contained in a cell made of polycrystalline sapphire [14] which is resistant to chemical reaction with Se at high temperatures. Two cells with sample thickness of 50  $\mu\text{m}$  and 100  $\mu\text{m}$  were prepared and hereafter we refer to them as Cell-50 and Cell-100, respectively. Cell-50 could be used for the measurements in the density region from semiconducting fluid to dense vapor around the critical point while Cell-100 was available for dense Se vapor. The temperature was measured at three locations by B-type thermocouples (Pt/Rh 30 % , Pt/Rh 6 %) and the difference of the temperatures was within 5  $^{\circ}\text{C}$  at 1650  $^{\circ}\text{C}$ . After liquid Se was loaded in the thin space of Cell-50 and Cell-100 at 500  $^{\circ}\text{C}$  and 1 bar, the vessel was pressurized up to 600bar. Then we increased and controlled temperature to measure XAFS spectra. When the temperature was increased to 1650  $^{\circ}\text{C}$ , the pressure was reduced to measure the spectra. Near the critical density,  $\rho_c$ , the pressure was decreased at intervals of 4 bar and the spectra were measured at each pressure.

### 3 Results

A standard procedure [15] was performed to deduce normalized XAFS oscillation,  $\chi(k)$ , where  $k$  is the wave-number of a photoelectron, from an x-ray absorption spectrum. Since an edge jump has a linear relation with the density of sample, x-ray absorption spectrum contains information on the density. By obtaining a scaling constant between Cell-50 and Cell-100 by comparing the edge jumps at the same temperature and pressure, the density,  $\rho$ , at the measured condition was estimated. The obtained scaling factor is about 3 because of the uncertainty in the sample thickness is estimated to be  $\pm 10\%$ .

Figure 1 shows  $\chi(k)$  of fluid Se at various temperatures and pressures together with the estimated  $\rho$ . The  $\chi(k)$  from 200 bar to 420 bar at 1650  $^{\circ}\text{C}$  were obtained using Cell-100 and the others using Cell-50. As shown in the figure a phase shift is observed between 430 bar and 434 bar at 1650  $^{\circ}\text{C}$ , where  $\rho$  increases across the isochore of  $\rho_c$ .

Figure 2 shows the magnitude of Fourier transform,  $|F(r)|$ , of  $k$  times  $\chi(k)$  shown in Fig. 1. The first peak around 2  $\text{\AA}$  in  $|F(r)|$  at 500  $^{\circ}\text{C}$  and 700  $^{\circ}\text{C}$  is approximately

symmetric. The peak position is shifted toward smaller  $r$  at 1230 °C where the SC-M transition occurs. A shift of the first peak is observed between 430 bar and 434 bar corresponding to the phase shift in  $\chi(k)$ .

## 4 Discussion

To investigate the quantitative variation of the bond length, a standard curve fit analysis is performed based on a one-Gaussian model [15].

$$k\chi(k) = S|f(\pi, k')|N_1 \exp(-2\sigma_1^2 k'^2 - 2r_1/\lambda(k')) \frac{\sin(2k'r_1 + \phi(k'))}{r_1^2}, \quad (1)$$

$$k' = \sqrt{k^2 - \Delta E_0/3.81}, \quad (2)$$

where  $|f(\pi, k)|$  and  $\phi(k)$  are the backward scattering amplitude and phase shift parameters for a Se atom calculated by FEFF code[16], respectively.  $N_1$ ,  $r_1$ , and  $\sigma_1$  are the coordination number, the bond length, and the mean-square displacement of  $r_1$  for Gaussian distribution function, respectively. A mean free path of a photoelectron,  $\lambda(k)$ , and a scaling factor adjusting an experimental backward scattering amplitude with the theoretical one,  $S$ , are estimated by the FEFF code.  $\Delta E_0$  is a correction of the absorption edge and it is optimized as a parameter in this analysis.

Figure 3 shows the optimized  $r_1$  and  $N_1$  as a function of  $\rho$ .  $r_1$  is denoted by solid symbols and  $N_1$  by open ones. The results from Cell-50 and Cell-100 are denoted by squares and circles, respectively. Both results agree well with in the error bar in the overlapping region at  $\rho < \rho_c$ . The optimized  $r_1$  and  $N_1$  values around  $\rho = 0.3$  g/cm<sup>3</sup> are about 2.15 Å and about 1, respectively. These results mean that most of Se atoms form Se dimers at this density. The increase of  $r_1$  shows linear dependence from 0.3 g/cm<sup>3</sup> to  $\rho_c$ . We call this region NM-1. When  $\rho$  exceeds  $\rho_c$ ,  $r_1$  increases from about 2.18 Å to more than 2.2 Å and the slope of its dependence on  $\rho$  increases significantly. This density region up to 2.8 g/cm<sup>3</sup> is named NM-2.

Let us compare the radial distribution function in NM-1 and NM-2. It is noteworthy that  $|F(r)|$  in NM-2 is asymmetric with a tail extending toward larger  $r$  while  $|F(r)|$  in NM-1 is approximately symmetric. However it may be difficult to deduce

the real atomic distribution from the asymmetrical peak in NM-2 because  $|F(r)|$  in NM-1, where the fluid consists mainly of Se dimers, shows a secondary peak on both sides of the first peak. To reduce such a noise, we assume that all the  $\chi(k)$  for cell-50 have the same systematic noise. We perform a Fourier back-transformation of the first peak at  $\rho = 1.3 \text{ g/cm}^3$ . By subtracting the back-transformed oscillation from the initial  $\chi(k)$ , a noise spectrum is deduced. Taking account of the difference between the edge jumps, we subtract the noise spectrum from the  $\chi(k)$  for other densities and deduce noise-reduced  $\chi(k)$ . The same procedure was tried for the spectra of Cell-100 but the noise was not reduced.

Figure 4 shows  $|F(r)|$  obtained from the noise-reduced  $\chi(k)$ . The first peak in  $|F(r)|$  of  $1.4 \text{ g/cm}^3$  is symmetric and the secondary peaks are reduced. The  $r_1$  obtained from the curve fit analysis is  $2.18 \text{ \AA}$ , which indicates that most of molecules in the fluid are Se dimers. When  $\rho$  exceeds  $\rho_c$ , the first peak in  $|F(r)|$  becomes asymmetric toward larger  $r$  and the asymmetry remains for every  $|F(r)|$  in NM-2. In the previous XAFS measurements [14], the obtained bond length around  $0.3 \text{ g/cm}^3$  is  $2.17 \pm 0.01 \text{ \AA}$ . The difference in the bond length is considered to be within uncertainties of the measurements.

We performed the curve fit analysis based on a two-Gaussian model [15] for the asymmetric first peaks in non-metallic dense vapor in NM-2 and the obtained bond lengths are  $2.18 \text{ \AA}$  and  $2.30 \text{ \AA}$ . Figure 5 shows the pair distribution function,  $g(r)$ , reproduced using the optimized structure parameters for f-Se just above and below  $\rho_c$ . The bond length of  $2.18 \text{ \AA}$  corresponds to that of a Se dimer. The length of  $2.30 \text{ \AA}$  is close to the bond distance in the metallic f-Se. These are the first data which show that the supercritical fluid in non-metallic region denser than  $\rho_c$  is a mixture of Se dimers and larger molecules.

It is interesting to review the structure in the SC and M region. We have carried out XAFS measurements for supercritical f-Se in SC-M transition region for the first time and the results have been published [10]. However the noise-reduced  $|F(r)|$  is first deduced in SC and M regions in the present analysis. As seen in Fig. 4, in SC region from  $3.7 \text{ g/cm}^3$  to  $3.5 \text{ g/cm}^3$  the first peak in  $|F(r)|$  is symmetric and the

optimized  $r_1$  is  $2.33 \pm 0.01 \text{ \AA}$ . When SC-M transition occurs around  $1200 \text{ }^\circ\text{C}$  the peak position is shifted to smaller  $r$  and the width becomes larger. We suggest that the optimized  $r_1$  at  $3.0\text{g/cm}^3$  in the M region is  $2.29 \pm 0.01 \text{ \AA}$  as shown in Fig. 3. These results are an indication that the intrachain covalent bond becomes stronger in the SC-M transition.

To discuss the structural change with SC-M-NM transition, it is useful to consider the results of a computer simulation. Shimojo et al.[13] performed ab initio molecular dynamics simulation for supercritical f-Se based on generalized-gradient-corrected density functional theory. Although they carried out the simulation at higher pressure than the present measurements, their results show that the first peak position in  $g(r)$  is shifted from  $2.35 \text{ \AA}$  in semiconducting fluid to  $2.32 \text{ \AA}$  in a metallic one with increasing the number of short chain molecules. Our XAFS results show a tendency similar to their results.

Recently they carried out similar simulation for dense Se vapor with  $1 \text{ g/cm}^3$  and  $2 \text{ g/cm}^3$  corresponding to NM-1 and NM-2, respectively, taking spin effects into account. Their results show that for f-Se in NM-1 most of molecules are Se dimers and the number of chain molecules is less than the number of dimers. The XAFS result shows that  $r_1$  increases with increasing  $\rho$  in NM-1. The simulation results suggest that this increase is due to the increasing number of chain molecules with increasing  $\rho$ . The simulation results in NM-2 show that most of Se atoms form chain molecules. On the other hand, our XAFS results that f-Se in NM-2 is a mixture of Se dimers and chain molecules are not consistent with the simulation. This difference may imply that in the dense vapor the effect of the density fluctuations increases the probability of forming Se dimers.

## 5 Conclusion

The dense Se vapor with the density below  $\rho_c$  of  $1.85 \text{ g/cm}^3$  mainly consists of Se dimers and the first peak of  $|F(r)|$  is symmetrical. With increasing density from  $0.3 \text{ g/cm}^3$  to  $1.4 \text{ g/cm}^3$  the average bond length of dense Se vapor becomes gradually longer. When the density exceeds  $\rho_c$ , the bond seems to elongate discontinuously

and the first peak in  $|F(r)|$  shows an asymmetrical pattern with a tail extending towards larger  $r$ . The peak is well reproduced using two-Gaussian peaks and the obtained distances are 2.18 Å and 2.30 Å, which suggests a mixture of Se dimers and chain molecules. Large density fluctuations and the strong intermolecular interaction may induce the formation of larger molecules around  $\rho_c$ , where the average distance between Se dimers is estimated to be 4.7 Å from a small angle x-ray scattering measurement [17]. The results of computer simulation by Shimojo et al. [?] is consistent with above idea.

## Acknowledgments

The authors are grateful to Professor Hoshino and Dr. Shimojo for their valuable discussion and indebted to Mr. R. Bruyere and Mr. O. Geaymond for their helpful technical support. This work is partly supported by the Grant-in-Aid for Scientific Research Fund from the Ministry of Education, Science and Culture of Japan, Electric Technology Research Foundation of Chugoku in Japan and a PICS support from CNRS in France.

## References

- [1] H. Hoshino, R. W. Schmutzler and F. Hensel, Ber. Bunsenges. Phys. Chem. 80, (1976) 27.
- [2] W. W. Warren, Jr. and R. Dupree, Phys. Rev. B22 (1980) 2257.
- [3] R. Fischer, R. W. Schmutzler and F. Hensel, J. Non-Cryst. Solids, 35/36 (1980) 1295.
- [4] M. Edeling and W. Freyland, Ber. Bunsenges. Phys. Chem., 85 (1981) 1049.
- [5] H.-P. Seyer, K. Tamura, H. Hoshino, H. Endo and F. Hensel, Ber. Bunsenges. Phys. Chem. 90 (1986) 587.
- [6] K. Tamura, J. Non-Cryst. Solids, 117/118 (1990) 450.
- [7] K. Tamura and S. Hosokawa, Ber. Bunsenges. Phys. Chem., 96 (1992) 681.

- [8] K. Tamura, J. Non-Cryst. Solids, 205-207 (1996) 239.
- [9] M. Inui, T. Noda, K. Tamura and C. Li, J. Phys.: Condens. Matter 8 (1996) 9347.
- [10] Y. Soldo, J. L. Hazemann, D. Aberdam, M. Inui, K. Tamura, D. Raoux, E. Pernot, J. F. Jal and J. Dupuy-Philon, Phys. Rev. B57 (1998) 258.
- [11] F. Kirchhoff, M. J. Gillan, J. M. Holender, G. Kresse and J. Hafner, J. Phys.: Condens. Matter 8 (1996) 9353.
- [12] S. Hosokawa, T. Kuboi and K. Tamura, Ber. Bunsenges. Phys. Chem. 101 (1997) 120.
- [13] F. Shimojo, K. Hoshino, M. Watabe and Y. Zempo, J. Phys.: Condens. Matter 10 (1998) 1199.
- [14] S. Hosokawa, K. Tamura, M. Inui, M. Yao, H. Endo and H. Hoshino, J. Chem. Phys., 97 (1992) 786.
- [15] B. K. Teo, *EXAFS: principles and data analysis*, Springer-Verlag, (1986).
- [16] J. J. Rehr, J. Mustre de Leon, S. I. Zabinsky and R. C. Albers, J. Am. Chem. Soc. 113 (1991) 5135.
- [17] M. Inui, I. Nakaso, Y. Oh'ishi and K. Tamura, J. Non-Cryst. Solids, in this volume.

## Figure Captions

- Figure 1            XAFS oscillation,  $\chi(k)$ , of f-Se.
- Figure 2            The magnitude of Fourier transform,  $|F(r)|$ , of  $k$  times  $\chi(k)$  shown in Fig. 2.
- Figure 3            The bond length  $r_1$  and the coordination number  $N_1$  obtained by curve fit analysis based on one Gaussian model.
- Figure 4            Noise-reduced  $|F(r)|$  for f-Se.
- Figure 5            The pair distribution function,  $g(r)$ , reproduced using the optimized  $N_1$ ,  $r_1$  and  $\sigma_1$  for f-Se.

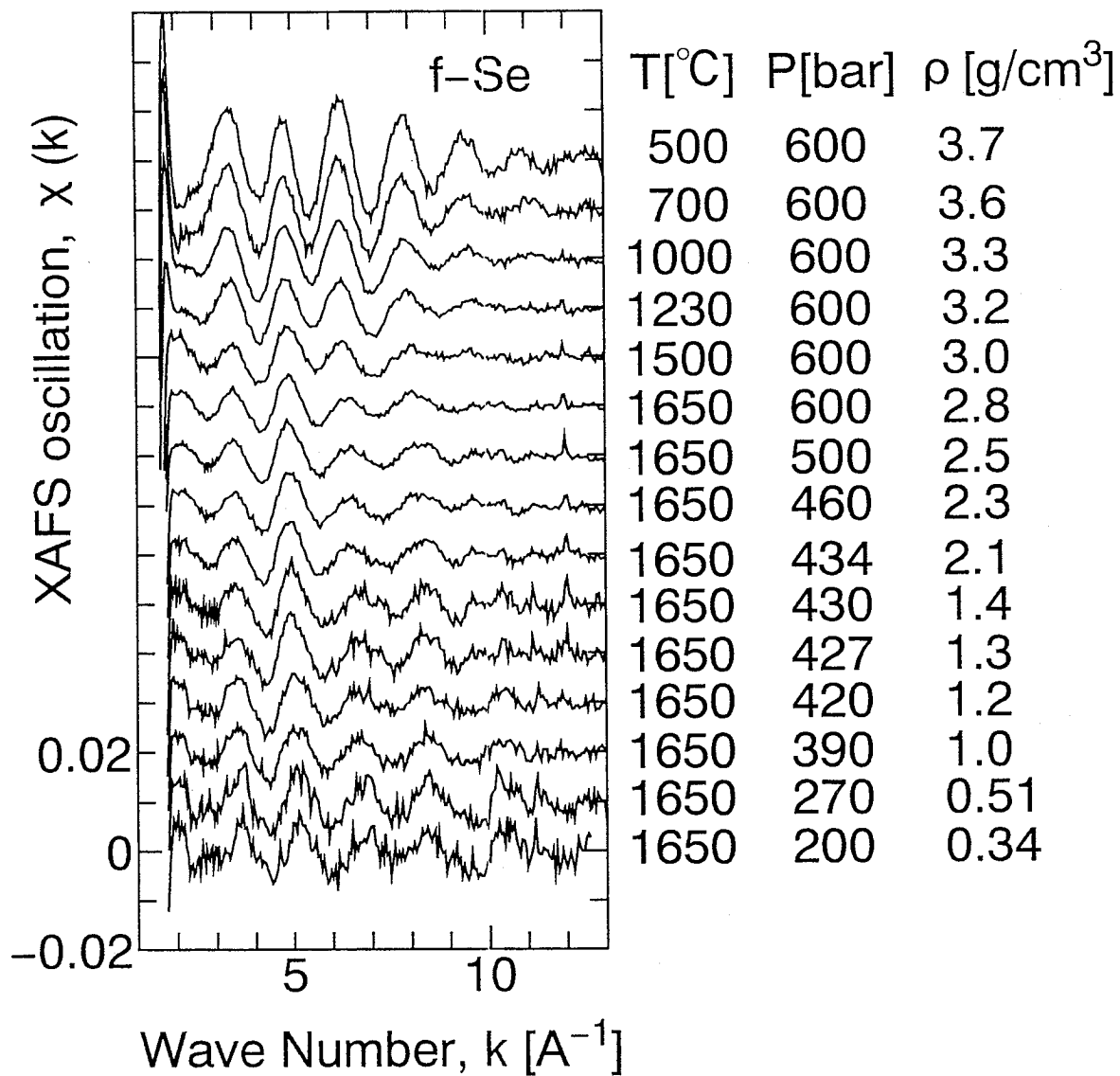


Fig.1

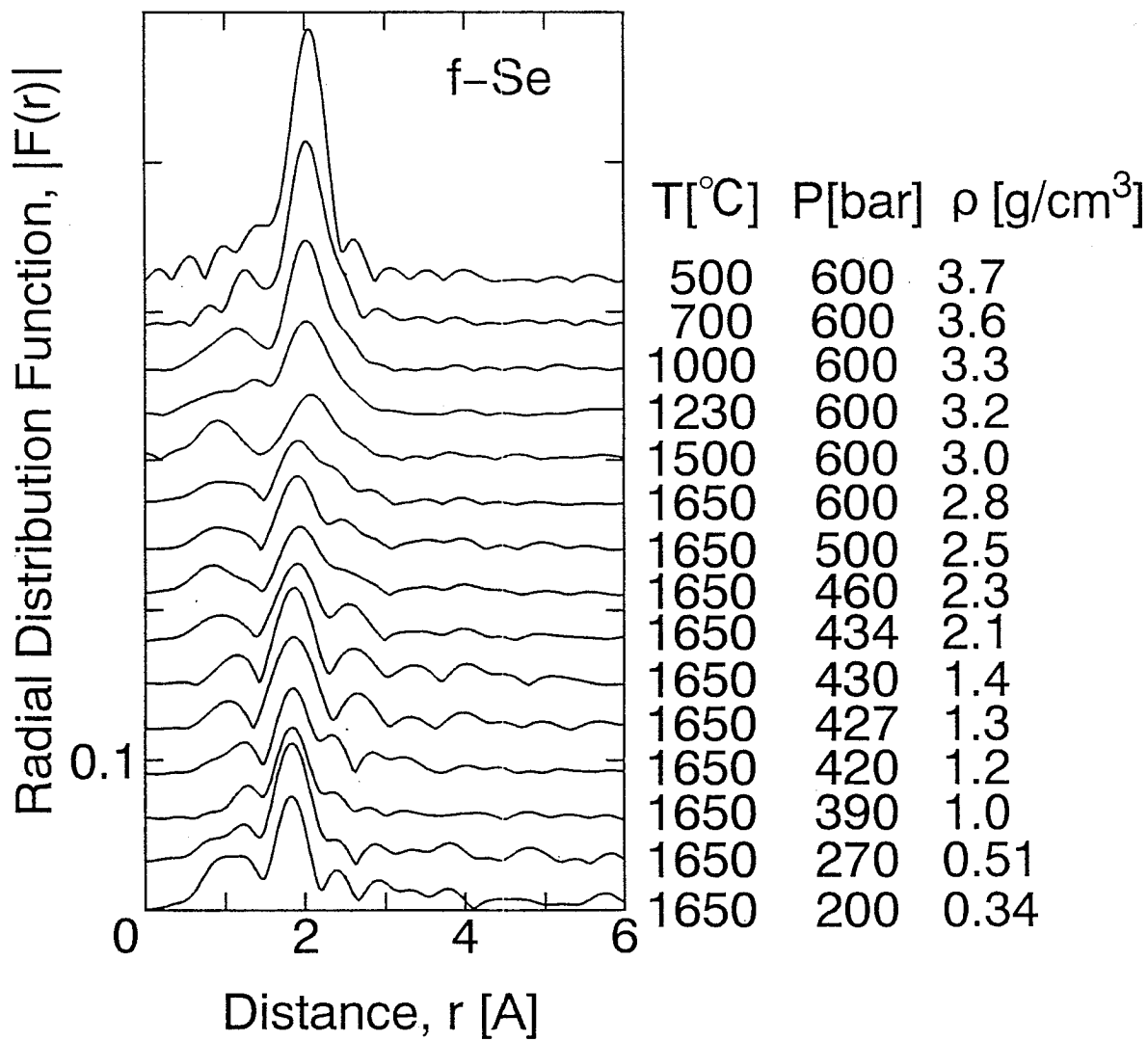


Fig.2

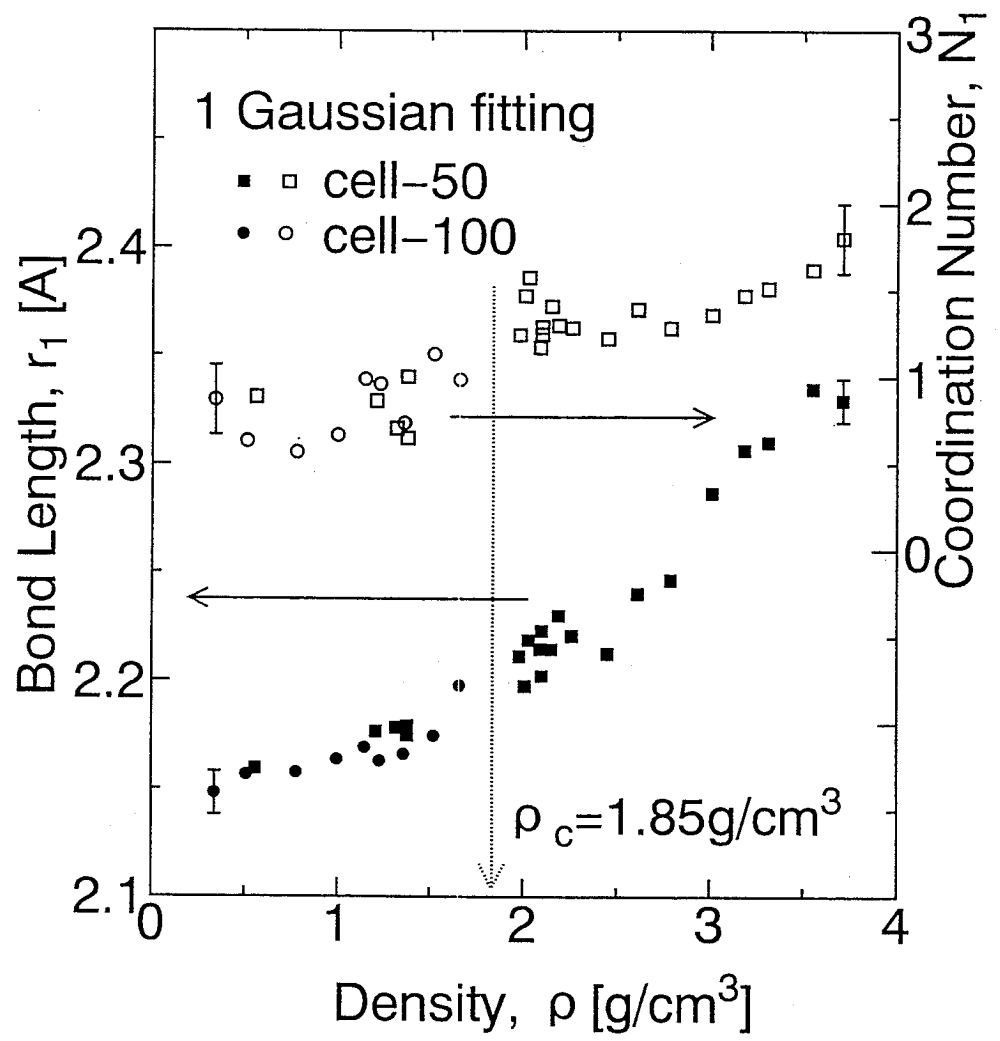


Fig.3

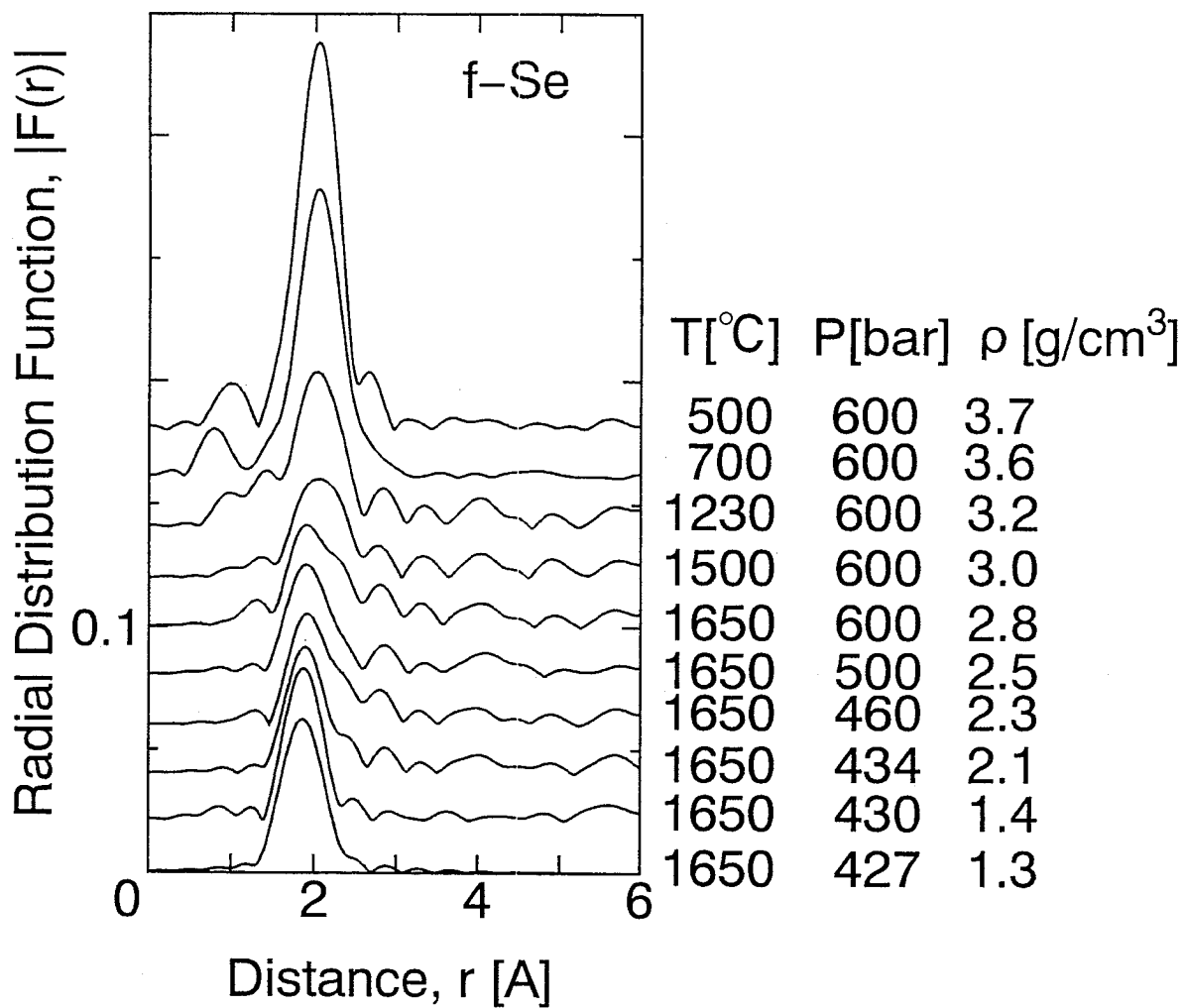


Fig.4

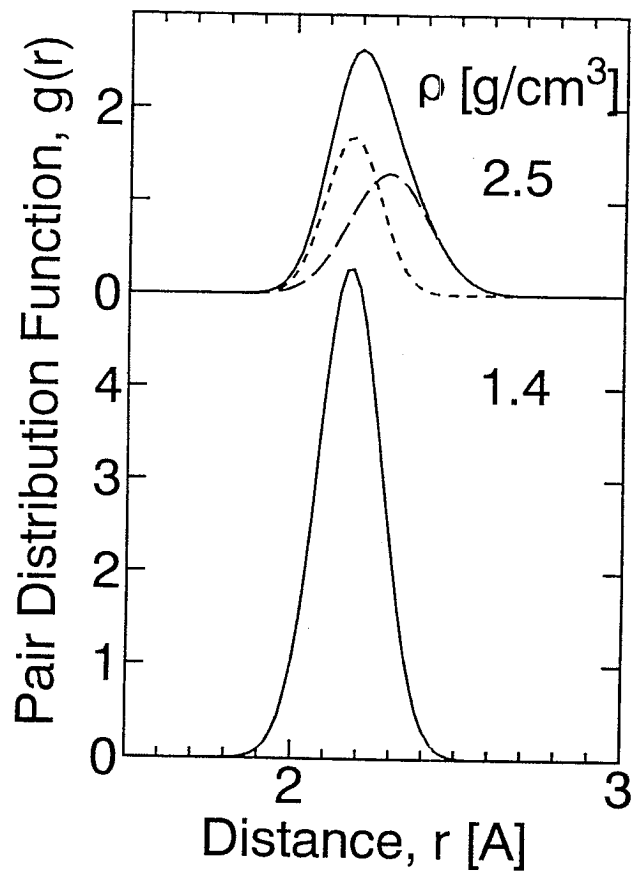


Fig.5